ACS OMEGA

http://pubs.acs.org/journal/acsodf

Article

# Endothermic Cracking of *n*-Dodecane in a Flow Reactor using Washcoated Activated Carbon on Metal Foam

Jeongin Mun, Nari Kim, Byunghun Jeong, and Jihoon Jung*

Cite This: *ACS Omega* 2022, 7, 8518−8525

Read Online

ACCESS | Metrics & More | Article Recommendations | Supporting Information

**ABSTRACT:** The heat generated by air friction during the flight of a hypersonic vehicle must be timely removed. For this purpose, a cooling technology based on the endothermic decomposition of the loaded fuel has been developed. In this study, the decomposition of *n*-dodecane was performed using activated carbon as a catalyst, which was coated onto metal foam to maximize the heat sink of the catalytic decomposition reaction. By applying this technology, the heat sink was increased to 1805 Btu/lb, and the gas yield was as high as 72%.

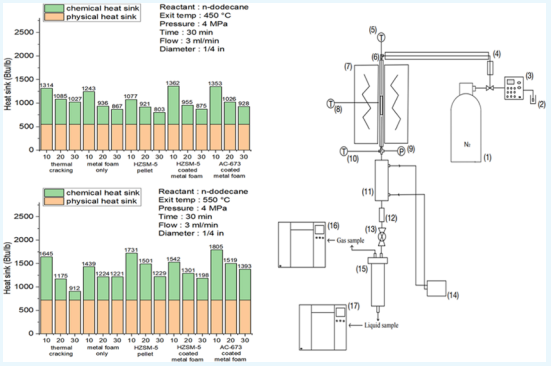


## 1. INTRODUCTION

During the flight of a hypersonic vehicle, the temperature of the aircraft surface reaches 3300 °C due to frictional heat, leading to serious problems such as structural deformation and electronic equipment failure.[1] Various cooling technologies using cryogenic or liquid hydrocarbon fuels have been developed to reduce the frictional heat of hypersonic vehicles. The methods based on cryogenic fuels (such as liquid hydrogen) require storage tanks with relatively high capacities due to the low density of these fuels, causing safety problems. To resolve this issue, cooling technologies using liquid hydrocarbon fuels have been proposed recently.[2−5] They involve several cooling approaches.[6,7] One approach is cooling by a physical endotherm (sensible heat), which represents a fixed amount of heat absorbed due to a temperature increase.[8] Another approach is cooling by a chemical endotherm that absorbs heat in the course of an endothermic reaction. The chemical endotherm derived from catalytic cracking and dehydrogenation can be enhanced by utilizing a proper catalyst.

Activated carbon (AC) is employed in various industrial applications because of its large surface area, low cost, and high thermal stability.[9−12] It is considered as an advanced catalyst for the catalytic cracking reaction, and the product yield is higher using activated carbon compared to that of the HZSM-5 catalyst.[13−17] In addition, the surface area of AC can be increased through physical treatment, and the formation of a microporous structure has been observed during a thermally activated process.[18,19] The walls between micropores burn out to form mesopores and reopen the blocked micropores.

Coke is produced during the endothermic reaction as a byproduct, and its amount increases due to the polymerization and condensation of the main products.[20−23] However, coke formation should be suppressed because it reduces the activity of the catalyst by blocking its surface pores. At the same time, the produced coke increases the pressure drop by blocking the fuel flow path and reduces the heat sink by acting as an insulating material. Therefore, a special technology must be developed to minimize the catalyst deactivation caused by coke formation.

Washcoating is widely used to coat a catalyst on a support by dehydrating the catalyst−support interface.[24−27] In this process, metal foams with large surface areas are often utilized as supports. However, very few studies on the use of metal foams as catalyst supports for endothermic reactions have been conducted previously.[28,29]

The purpose of this work was to determine the heat sink of a liquid hydrocarbon fuel decomposition reaction performed in a flow reactor using a coated catalyst and develop an effective coating method.

## 2. RESULTS AND DISCUSSION

### 2.1. Temperature-Programmed Desorption Studies.

Figure 1 displays the $NH_3$-temperature-programmed desorp-

Received: November 8, 2021
Accepted: February 18, 2022
Published: March 2, 2022

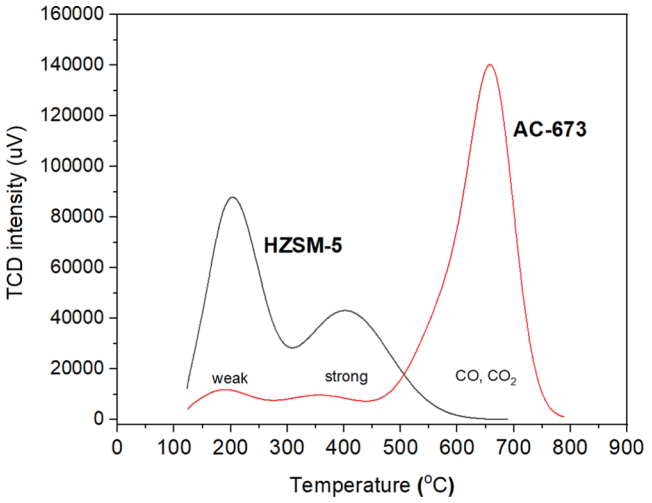


**Figure 1.** $NH_3$-TPD profiles of the HZSM-5 and AC-673 catalysts.

tion (TPD) profiles with a thermal conductivity detector (TCD) detector, and Figure 2 displays the $NH_3$-TPD with an

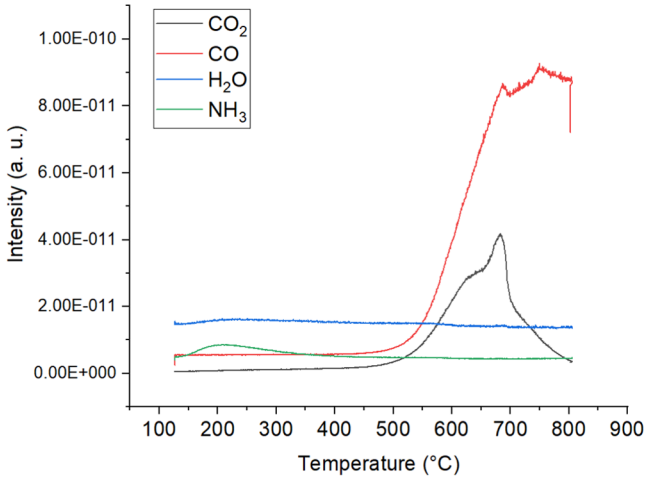


**Figure 2.** $NH_3$-TPD with an MS detector profile of the AC-673 catalysts.

mass spectrometer (MS) detector. Figure 1 shows the presence of three different types of profiles on their surfaces: weak acidic site (100−300 °C), strong acidic site (300−500 °C), and carbon monoxide and carbon dioxide (500−800 °C). The HZSM-5 sample contained weak and strong acid sites. However, the activated carbon sample contained a small amount of weak acid sites because there is some $NH_3$ desorption in Figure 2. The weak acid sites of AC consisted of many functional groups such as carboxyl, hydroxyl, ether, carbonyl, ketone, etc. The OH, C−N, and C−O−C functional groups presented on carbon were the factors that affect the catalytic cracking.[30] Since the carbon contained many elemental compounds and active sites, the hydrocarbon fuel contact with functional groups to undergo a cleavage reaction. Moreover, the yield of the gas product could be higher through the contribution of the radical mechanism at a high reaction temperature. As shown in Figure 2, the large peak at 650 °C was assigned to the decomposition of activated carbon to form carbon monoxide and carbon dioxide from the result of $NH_3$-TPD with an MS detector.

**2.2. Cracking Reaction of *n*-Dodecane.** *2.2.1. Gas Yields and Product Composition.* Figure 3 shows the gas yield

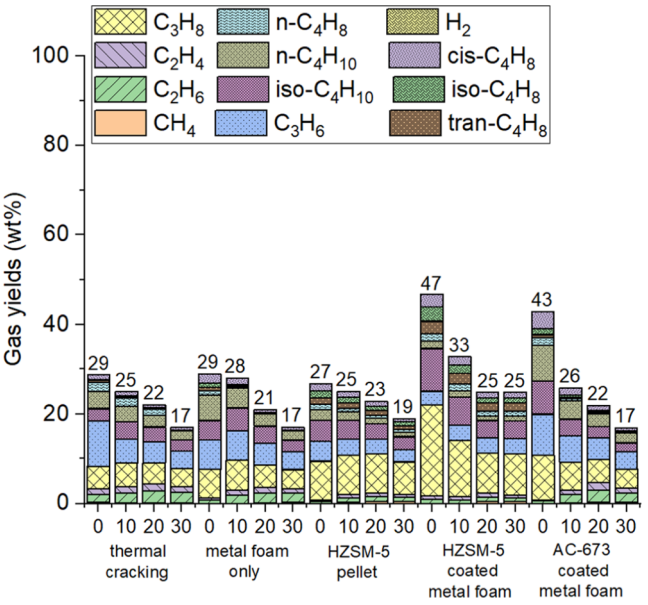


**Figure 3.** Gas yields and product compositions obtained after 0, 10, 20, and 30 min of reaction at a temperature of 450 °C and pressure of 4 MPa.

values obtained during the thermal and catalytic cracking of *n*-dodecane at a temperature of 450 °C and pressure of 4 MPa. Note that the gas yield is directly related to the corresponding endotherm, and the maximum heat sink is obtained for the endothermic fuel when its entire amount is fully converted into gas products. Theoretically, the chemical heat sink of *n*-dodecane completely converted to ethylene ($C_2H_4$) is 1530 Btu/lb.[3] In reality, the gas products (from $CH_4$ to $C_4H_8$) considerably increase their value. Furthermore, the heat sink increases as the enthalpy of the gas product increases. The enthalpies of the obtained products are ranked in the following order: $H_2$ > $C_2H_4$ > $C_3H_6$ > *cis*-$C_4H_8$ > *n*-$C_4H_8$ > *trans*-$C_4H_8$ > iso-$C_4H_8$ > $CH_4$ > $C_2H_6$ > $C_3H_8$ > *n*-$C_4H_{10}$ > iso-$C_4H_{10}$. However, the enthalpy differences between various gas products are insignificant, and the total gas yield predominantly affects the heat sink.

The 0 min sample was taken immediately after the beginning of the reaction. The other samples were collected at 10 min intervals. Note that the gas products are favorable for an endothermic reaction because gas formation enthalpies are relatively high. At 0 min of each reaction, the highest gas yield values were achieved for HZSM-5/metal foam (47 wt %) and AC-673/metal foam (43 wt %). The next gas yield value of 29 wt % was obtained for both thermal cracking and metal foam only. Its magnitude was relatively low because the corresponding processes did not involve catalysts. The stainless-steel tube and metal foam could act as metal catalysts; however, their efficiencies at 450 °C were very low (a temperature of 500 °C or higher is typically required to activate metal catalysts). The lowest gas yield of 27 wt % was obtained for the HZSM-5 pellet with small heat transfer efficiency due to the low reaction temperature. After 10 min of reaction, the gas yield of HZSM-5/metal foam was 33 wt % and that of the AC-673/metal foam sample was 26 wt %, indicating rapid catalyst deactivation. Unlike the coated catalysts, no rapid deactivation was observed


https://doi.org/10.1021/acsomega.1c06272
ACS Omega 2022, 7, 8518−8525

for the other systems. The gas yield of HZSM-5/metal foam was 25 wt %, and this value remained stable for 30 min. The gas yield of the HZSM-5 pellet decreased to 19 wt % after 30 min of reaction, but the other yield values decreased to 17 wt %. As a result, the gas yield of the HZSM-5/metal foam sample had the maximum values.

Figure 4 shows the gas yields and product compositions obtained during the thermal and catalytic cracking of *n*-dodecane at 550 °C and 4 MPa. At the beginning of the reaction, the gas yield of AC-673/metal foam was as high as 72 wt %. For a chemical endotherm, the heat sink proportionally increases with an increase in the gas yield due to the high enthalpy of product formation. The gas yield of the metal foam only was 64 wt % because the foam acted as a metal catalyst at a temperature of 550 °C. The gas yield of the HZSM-5/metal foam sample was 60 wt % and that of the HZSM-5 pellet was 58 wt %. As the large surface area of the metal foam promotes the heat and mass transfer between the fuel and the catalyst, HZSM-5/metal foam had a higher gas yield than that of the HZSM-5 pellet. Finally, the yield obtained during the thermal cracking was 52 wt %. At a high temperature of 550 °C, both the catalyst and metal demonstrated higher gas yields than that of thermal cracking, owing to their high catalytic efficiencies. After 10 min of reaction, the gas yield of the HZSM-5 pellet was 55 wt %, and its deactivation proceeded very slowly; however, the yield values of AC-673/metal foam, HZSM-5/metal foam, and metal foam only samples were drastically reduced. After 20 min of reaction, the gas yield of the HZSM-5 pellet slightly decreased to 47 wt %. Meanwhile, the yield of HZSM-5/metal foam was 36 wt %, and its deactivation occurred much faster. After 30 min of reaction, the yields of both the AC-673/metal foam and HZSM-5 pellet samples were 42 wt %. The yield of the HZSM-5/metal foam catalyst was 32 wt %, which was much lower than the value obtained for thermal cracking. As the packed HZSM-5/metal foam lost most of its initial catalytic activity, it drastically reduced the space-time by occupying the reaction space.

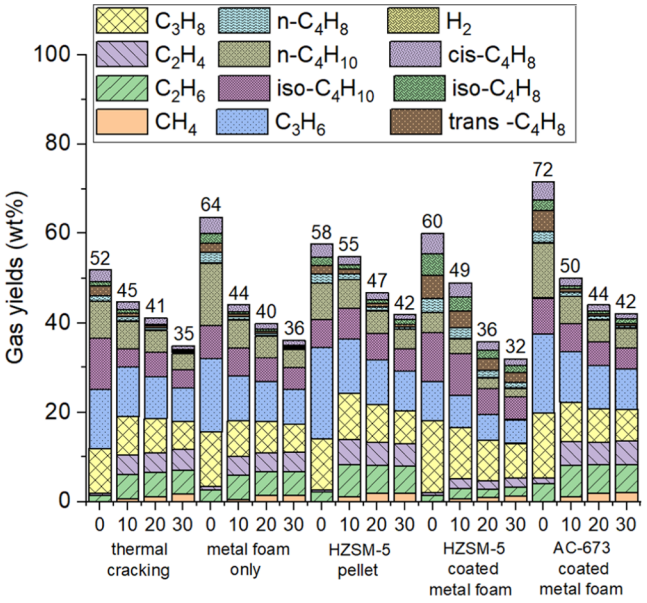


**Figure 4.** Gas yields and product compositions obtained after 0, 10, 20, and 30 min of reaction at a temperature of 550 °C and pressure of 4 MPa.

*2.2.2. Liquid Yields and Product Composition.* Figure 5 shows the liquid yields obtained during the thermal and catalytic cracking of *n*-dodecane at a temperature of 450 °C and pressure of 4 MPa. Unlike the gas products, the liquid products did not considerably increase the heat sinks due to their lower enthalpies of formation. However, the liquid products promoted the coke formation, as discussed in detail in the the following sections. The produced liquids were separated into linear paraffin, linear olefin, cyclic paraffin, cyclic olefin, a benzene/toluene/xylene (BTX) mixture, and naphthalene. In terms of cooling efficiency, BTX and naphthalene favor endothermic reactions as they exhibit high enthalpies of formation and can undergo dehydrogenation through the polymerization of their benzene rings. After three or more benzene rings are polymerized, their endotherms increase considerably. Although these compounds help increase the heat sink, they also serve as precursors to coke formation (as stated in the Introduction section, the amount of coke must be reduced because it blocks the fluid path and acts as an insulator that prevents heat transfer).

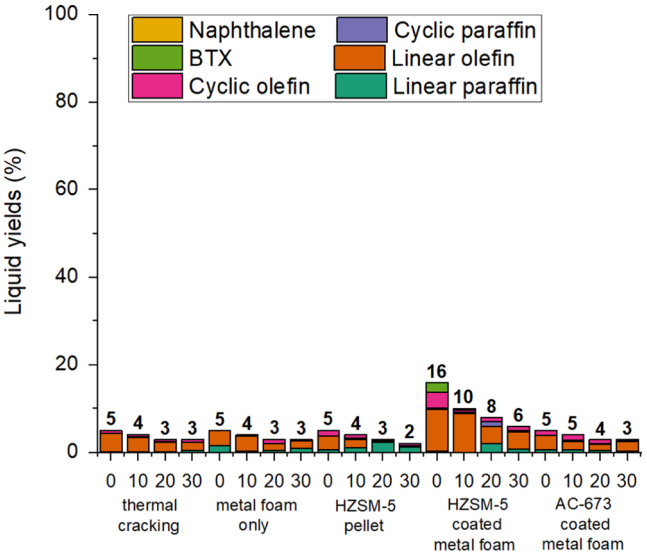


**Figure 5.** Liquid yields and product compositions obtained after 0, 10, 20, and 30 min of reaction at a temperature of 450 °C and pressure of 4 MPa.

Among the liquid yields presented in Figure 5, the yield of linear olefin was dominant, and naphthalene was not produced in every sample. BTX was formed at 0 min of the HZSM-5/metal foam reaction with a yield value of 2%. Linear paraffin, which has a higher molecular weight than *n*-dodecane, was formed via an exothermic reaction. As the HZSM-5 pellet predominantly produced linear paraffin after 20 and 30 min, its predicted heat sink was very low. Furthermore, after 30 min of reaction catalyzed by the HZSM-5 pellet, tetradecane ($C_{14}H_{30}$) was dominantly formed in the liquid sample. Thus, the HZSM-5 pellet possessed the lowest heat sink among the studied systems (see Figure 7).

Figure 6 shows the liquid yields obtained during the thermal and catalytic cracking of *n*-dodecane at a temperature of 550 °C and pressure of 4 MPa. As naphthalene possessed the highest endothermic capacity, the obtained endotherms decreased in the order of naphthalene > BTX > cyclic olefin > linear olefin > cyclic paraffin > linear paraffin. Every sample produced BTX at the early stage of the reaction. Among them,


https://doi.org/10.1021/acsomega.1c06272
ACS Omega 2022, 7, 8518−8525

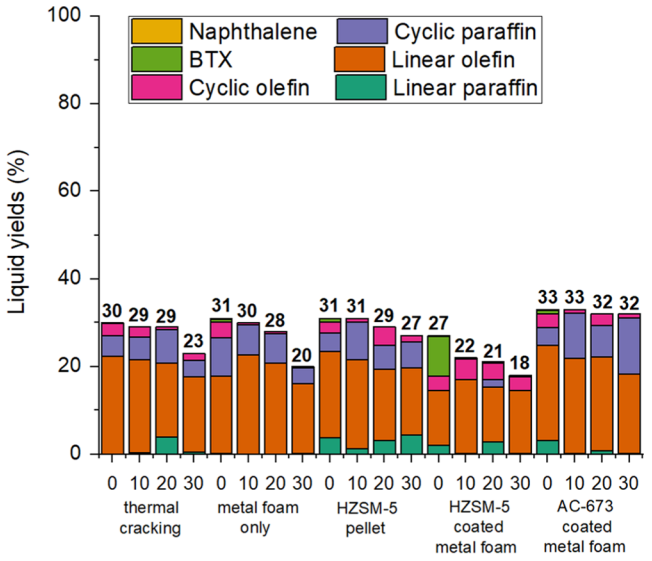


**Figure 6.** Liquid yields and product compositions obtained after 0, 10, 20, and 30 min of reaction at a temperature of 550 °C and pressure of 4 MPa.

HZSM-5/metal foam generated 9% BTX. HZSM-5/metal foam produced little cyclic paraffin although its considerable amounts were formed during the other reactions. As cyclic olefin was a precursor of aromatic compounds, it continuously generated a small amount of BTX in the reaction involving HZSM-5/metal foam. It is noteworthy that the liquid yield of AC-673/metal foam was maintained at 32% even after 30 min of reaction. Because the heat sink cannot be determined exclusively from the gas and liquid yields, its values were measured with the watt meter in the next section.

*2.2.3. Heat Sinks of n-Dodecane Cracking Reaction.* Figure 7 shows the heat sinks generated by the thermal and catalytic cracking of *n*-dodecane at a temperature of 450 °C and pressure of 4 MPa. As the heat sink is directly related to the utilized aircraft cooling technology, it should be carefully considered. The measured heat sink values were averaged over

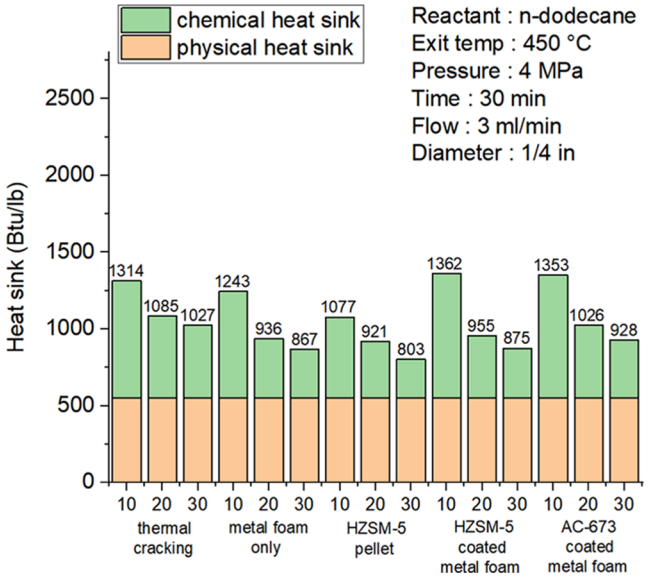


**Figure 7.** Average endotherms determined every 10 min of reaction at a temperature of 450 °C and pressure of 4 MPa using the watt meter.

a period of 10 min, and watts were converted to Btu/lb units by dividing them by the mass flow rate. After 10 min of reaction, the heat sinks of the HZSM-5/metal foam and AC-673/metal foam samples were 1362 and 1353 Btu/lb, respectively. Both catalysts exhibited high heat sinks during 10 min. The initial heat sinks of the metal foam only and HZSM-5 pellet were 1243 and 1077 Btu/lb, respectively. The heat sink of the reaction involving the metal foam only was lower than that of thermal cracking. As the reaction temperature was low, the foam did not act as a metal catalyst and occupied the reaction space for 30 min. The HZSM-5 pellet resulted in the lowest heat sink within the first 30 min of reaction because of the low gas yield and a large amount of produced linear paraffin. In contrast, the heat sink of thermal cracking was maintained at a high value for 30 min. Thus, at a low reaction temperature, both the acid and metal catalysts exhibited low catalytic efficiency and occupied the reaction space.

Figure 8 shows the heat sinks obtained during the thermal and catalytic cracking of *n*-dodecane at a temperature of 550

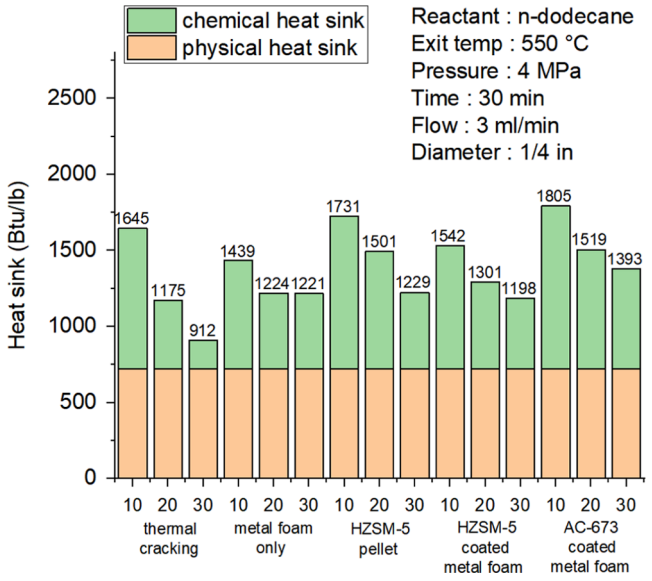


**Figure 8.** Average endotherms estimated every 10 min of reaction at a temperature of 550 °C and pressure of 4 MPa using the watt meter.

°C and pressure of 4 MPa. After 10 min of reaction, the heat sinks of the AC-673/metal foam and HZSM-5 pellet samples were 1805 and 1731 Btu/lb, respectively. The heat sink of AC-673/metal foam remained high for 30 min due to the high gas and liquid yield values. The heat sinks of the HZSM-5/metal foam and metal foam only samples were 1542 and 1439 Btu/lb, respectively. The heat sink of thermal cracking was 1645 Btu/lb at the initial reaction stage and rapidly decreased within the first 30 min of reaction. Note that the minimum heat sink that enables a hypersonic flight (Mach 8) is 1300 Btu/lb.[31] Because the heat sink of AC-673/metal foam exceeded 1300 Btu/lb for 30 min, this catalyst can be potentially commercialized.

**2.3. Coke Formation Analysis.** *2.3.1. Coke Amount.* Figure 9 shows the coke formation during the thermal and catalytic cracking of *n*-dodecane at a temperature of 450 °C and pressure of 4 MPa, which is measured by weighing reactor components before and after the reaction. The size of the filter was 2 $\mu$m, and the filter was dried at 250 °C for 30 min to


https://doi.org/10.1021/acsomega.1c06272
ACS Omega 2022, 7, 8518−8525

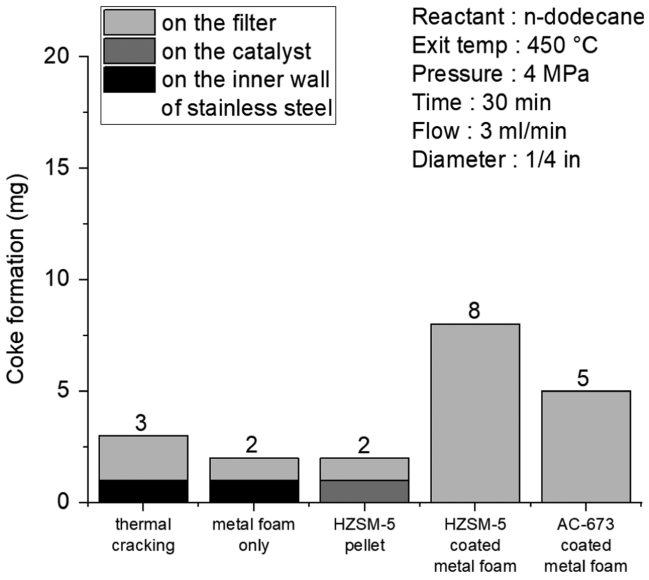


**Figure 9.** Coke formation during each reaction conducted at a temperature of 450 °C and pressure of 4 MPa.

evaporate the remaining *n*-dodecane after the reaction. The coke formed on the catalyst surface and on the inner wall of the stainless-steel tube could block the flow path and lead to aircraft explosion. A more serious problem was the coke produced on the stainless-steel tube wall (depicted by the black color in Figure 9). The coke amounts formed on the filters of the HZSM-5/metal foam and AC-673/metal foam catalysts were 8 and 5 mg, respectively. Because the higher gas yield increased the intensity of the Diels–Alder reaction, a larger amount of coke was produced using the HZSM-5/metal foam catalyst.[31−33]

Figure 10 shows the coke formation during the thermal and catalytic cracking of *n*-dodecane at a temperature of 550 °C and pressure of 4 MPa. The coke amounts produced using the AC-673/metal foam and metal foam catalysts were 35 and 21 mg, respectively. These high amounts resulted from the high

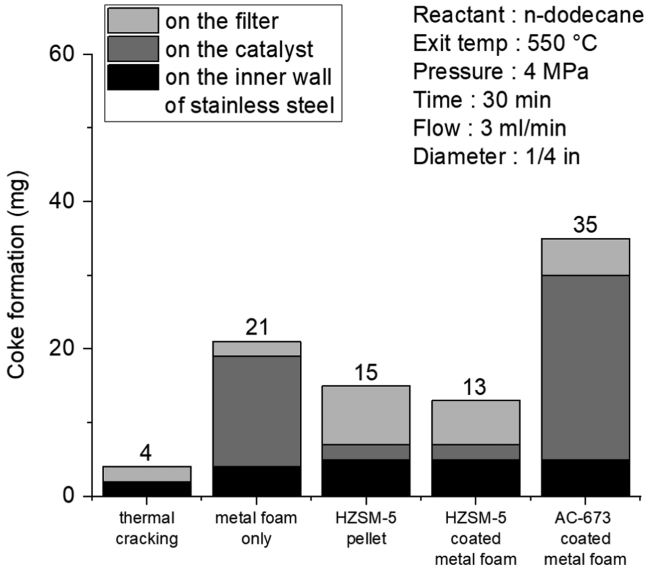


**Figure 10.** Coke formation during each reaction conducted at a temperature of 550 °C and pressure of 4 MPa.

gas yield values obtained for both catalysts. The coke formations of the HZSM-5 pellet and HZSM-5/metal foam were 15 and 13 mg, respectively. Thus, the coke formation on the HZSM-5/metal foam catalyst was significantly reduced by washcoating the HZSM-5 catalyst as compared with the value obtained for the metal foam only.

*2.3.2. Scanning Electron Microscope/Energy-Dispersive Spectroscopy (SEM/EDS) Analysis.* Figure 11 shows the SEM images of catalysts before the reaction, catalysts after the 450 °C reaction, and catalysts after the 550 °C reaction. There is no significant change in the catalyst morphology. The stability of the catalyst has been maintained after the 450 and 550°C reaction. As stated above, AC-673/metal foam which performed the highest heat sink at the temperature of 550 °C generated the highest coke amount. Among the cokes, the coke on the catalyst was the highest in Figure 10. In this case, it is needed to figure out that the coke on the catalyst had blocked the pore of metal foam. It was confirmed that the pore of metal foam was not blocked in Figure 11 (image d-3).

Table S1 presents the energy-dispersive spectroscopy (EDS) data obtained for the metal foam before the endothermic reaction and after the reactions conducted at 450 and 550 °C. Before the reaction, the carbon content was not measured, and 44% of oxygen species were detected in the form of a natural oxide film produced via the reaction with air oxygen species. Briefly, 21% of Cr atoms were detected in the Cr-based metal foam, and the amount of metals decreased in the order of Cr > Ni > Al > Fe. The atomic fractions of carbon obtained for the reactions conducted at 450 and 550 °C were 24 and 76%, respectively. The amount of coke production increased by approximately three times due to the high temperature. Table S2 lists the EDS data obtained for the HZSM-5 pellet before the reaction and after the reactions conducted at 450 and 550 °C. Here, O, Si, and Al elements were analyzed because HZSM-5 was composed of $SiO_2$ and $Al_2O_3$. The amounts of C in the reactions performed at 450 and 550 °C were 19 and 21%, respectively, indicating that the coke production increased with the reaction temperature. Table S3 presents the EDS data obtained for the HZSM-5/metal foam catalyst before the reaction and after the reactions conducted at 450 and 550 °C. The O and Si elements were predominantly detected due to the washcoating of HZSM-5 onto the metal foam, and the concentrations of the metal components did not exceed 2%. The amount of C increased from 17 to 29% due to the temperature increase; however, the contents of the other elements either decreased or remained constant. Table S4 lists the EDS data obtained for the AC-673/metal foam catalyst before the reaction and after the reactions conducted at 450 and 550 °C. The contents of C and O elements equal to 37 and 36%, respectively, were observed before the endothermic reaction due to the presence of oxidized AC. The Si amount was 5% because the washcoating process involved the silica binder. The amount of C increased from 47 to 85% as the reaction temperature increased; however, the contents of the other elements decreased. As a result, the coke production increased for all catalysts because of the high reaction temperature of 550 °C.

## 3. CONCLUSIONS

Thermal cracking without a catalyst, a reaction catalyzed by the metal foam, and a reaction catalyzed by the metal foam coated with a catalyst were conducted for *n*-dodecane inside a flow reactor. The maximum heat sink of the AC-673/metal foam


https://doi.org/10.1021/acsomega.1c06272
ACS Omega 2022, 7, 8518−8525

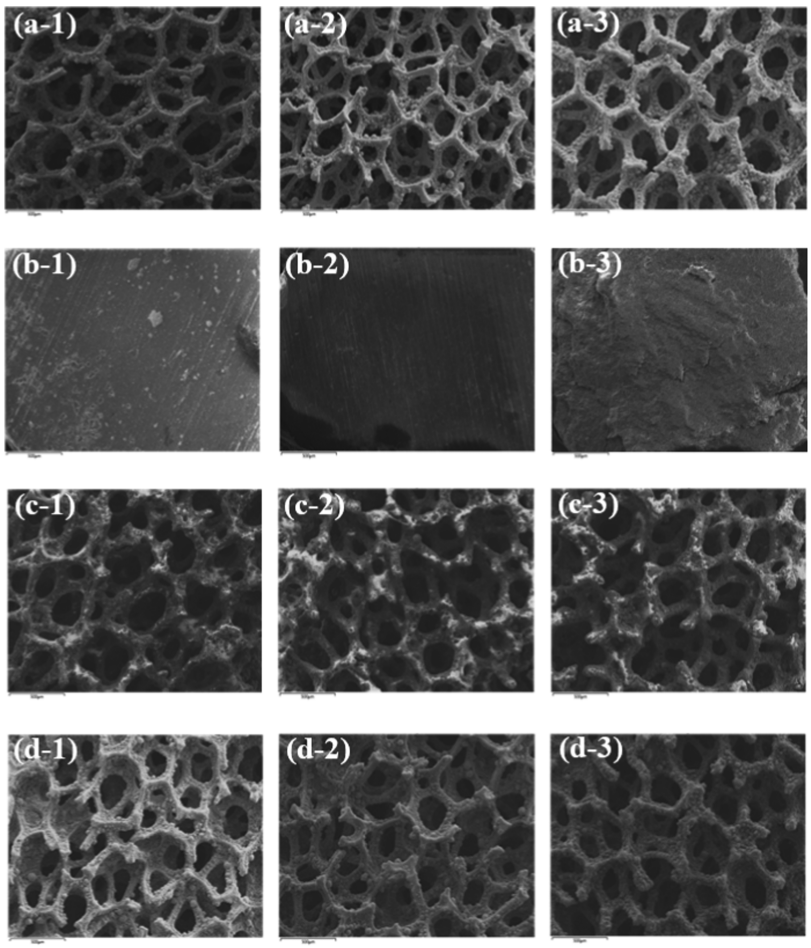


**Figure 11.** SEM images of the (a) metal foam catalyst, (b) HZSM-5 pellet catalyst, (c) HZSM-5/metal foam catalyst, and (d) AC-673/metal foam catalyst, magnification = ×50: catalysts before the reaction (a-1, b-1, c-1, d-1), catalysts after the 450 °C reaction (a-2, b-2, c-2, d-2), and catalysts after the 550 °C reaction (a-3, b-3, c-3, d-3).

sample was 1805 Btu/lb, and its gas yield was 72%. However, this catalyst also generated a high coke amount of 35 mg. As a result, the heat sink and gas yield values obtained for the AC-673/metal foam system were higher than those of the pellet catalyst.

## 4. EXPERIMENTAL SECTION

**4.1. Materials.** The $NH_3$-ZSM-5 zeolite (CBV-2314, $SiO_2$/$Al_2O_3$ mole ratio = 23) catalyst was purchased from Zeolyst. AC (untreated, granular, 20−60 mesh) and colloidal silica binder (LUDOX AS-30, 30 wt % suspension in $H_2O$) were purchased from Sigma-Aldrich. AC was oxidized in air as follows.[18] First, the bare AC was sieved between 30−50 mesh and then air-treated for 2 h at a temperature of 400 °C and a heating rate of 5 °C/min (further denoted as AC-673). Polyvinylpyrrolidone dispersion was purchased from TCI, and a Ni−Fe−Cr−Al metal foam support (N10 #05 model) was obtained from Alantum Co. A representative endothermic fuel, *n*-dodecane (98%, GR grade), was purchased from Kanto Chemical.

**4.2. Preparation of an HZSM-5 Pellet and Catalyst Coating Procedure.** $NH_3$-ZSM-5 powder was compressed at a pressure of 8 tons into a cylinder with a diameter of 3 mm and a height of 3 mm. The obtained pellet with a weight of approximately 20 mg was calcined at 550 °C for 5 h to produce HZSM-5, a catalytically active material (it was impossible to fabricate an AC pellet due to its high fragility caused by the low surface energy).

The metal foam was cut into a piece with a width of 3 mm and a length of 50 mm, which was subsequently cleaned with acetone for 15 min in an ultrasonic cleaner. The slurry utilized for ZSM-5 washcoating contained 6 wt % of the silica binder, 12 wt % of $NH_3$-ZSM-5, and 82 wt % of distilled water. The slurry for AC washcoating contained 1 wt % of the dispersion, 2 wt % of the silica binder, 2 wt % of AC, and 95 wt % of ethylene glycol. Each slurry was thoroughly mixed for 2 h. The prepared metal foam specimen was immersed into a slurry for 10 s, air-blown at 2.5 bar, and dried in an oven for 30 min at 150 °C. The dried metal foam was immersed into the same slurry for 10 s and dried again in an oven for 30 min. The number of washcoating cycles performed to load 40 mg of a catalyst was 5 for HZSM-5 and 10 for AC-673. The $NH_3$-ZSM-5 zeolite washcoated onto the metal foam was calcined at 550 °C for 5 h to generate HZSM-5 (further denoted as HZSM-5/metal foam), and the AC washcoated onto the metal foam was calcined at 400 °C for 2 h (further denoted as AC-673/metal foam).

**4.3. Endothermic Cracking Reaction.** A schematic of the utilized flow reactor is shown in Figure 12. The heat sink was measured every second using a watt meter. In addition, the heat loss (the amount of heat consumed in the reactor to


https://doi.org/10.1021/acsomega.1c06272
ACS Omega 2022, 7, 8518−8525

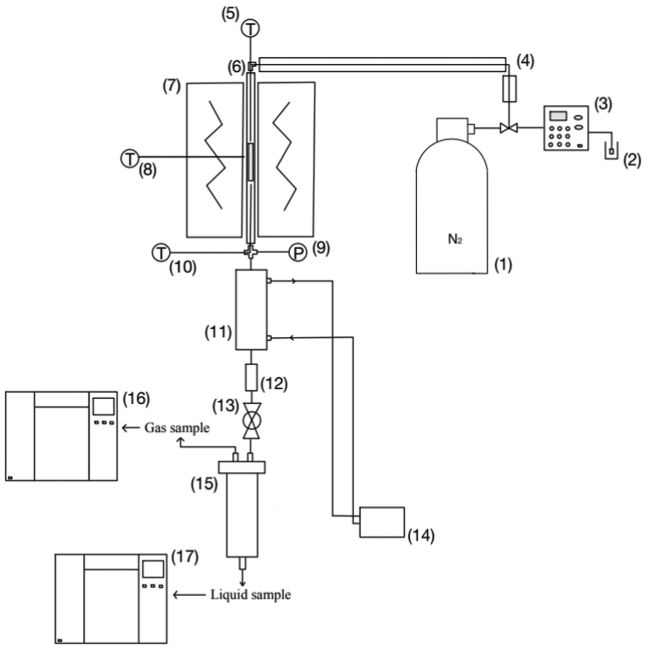


**Figure 12.** Experimental apparatus used for conducting the endothermic reaction: (1) N2 gas cylinder, (2) dodecane container, (3) pump, (4) preheater, (5) thermocouple, (6) tube reactor, (7) electrical heater, (8) thermocouple, (9) pressure sensor, (10) thermocouple, (11) condenser, (12) filter, (13) backpressure regulator, (14) cooler, (15) gas−liquid separator, (16) GC−FID, and (17) GC−MS.

maintain a required temperature) was subtracted from the measured energy value to obtain the exact heat sink.

The *n*-dodecane liquid fuel has a chain structure with a chemical formula of $C_{12}H_{26}$, a boiling point of 216 °C, and a critical point corresponding to a temperature of 385 °C and pressure of 1.8 MPa.[34] The preheater temperature was set to 300 °C at a fluid exit temperature of 450 °C and to 400 °C at a fluid exit temperature of 550 °C. The pressure in the reactor was 4 MPa. An endothermic reaction was conducted above the supercritical point. The reaction temperature and pressure were selected to simulate the hypersonic vehicle conditions. An additional experiment was performed at a fluid exit temperature of 650 °C, however, the fuel path was plugged as soon as the fuel reached the reaction area.

The flow reactor was first cleaned with acetone and then purged with nitrogen. The catalyst was packed inside the reactor, and the nitrogen pressure was adjusted to 4 MPa using a backpressure regulator. The decomposition reaction was conducted for 30 min at a flow rate of 3 mL/min using *n*-dodecane as the reactant. Gas and liquid samples were collected every 10 min during the reaction. The decomposition reactions conducted for *n*-dodecane included thermal cracking without a catalyst, a decomposition reaction using the pure metal foam, and catalytic decomposition reactions using the pellet and metal foam coated with HZSM-5 or AC-673. The reactor was fabricated from stainless steel and had an outer diameter of 6.35 mm, an inner diameter of 4.57 mm, and a length of 360 mm. As the catalytic reaction length was set to 100 mm in the middle of the furnace, the length of the packed metal foam was also 100 mm, and the weights of the loaded catalyst on the metal foam and packed pellet were approximately 40 mg each.

**4.4. Product Analysis.** The gaseous product yield was measured as the weight difference between the injected liquid fuel and discharged liquid fuel. The gas sample was analyzed using a gas chromatographer (GC, Agilent 6890N, Gaspro column) with a flame ionization detector (FID) and another GC (Agilent 6890N, molecular sieve 13X column) with a thermal conductivity detector (TCD). Gaseous hydrocarbon products were examined by the FID while increasing the oven temperature from 50 to 120 °C. The produced hydrogen gas was analyzed by the TCD at a fixed oven temperature of 50 °C. The liquid sample was analyzed using an Agilent 6890N GC equipped with an HP-5ms UI column and an Agilent 5975A mass spectrometer (MS) in the temperature range from 50 to 290 °C. A JEOL scanning electron microscope (SEM, JSM−7610F PLUS) was utilized operating at an acceleration voltage of 15 kV to analyze the elements of the catalyst and coke.

## ■ ASSOCIATED CONTENT

### Supporting Information

The Supporting Information is available free of charge at https://pubs.acs.org/doi/10.1021/acsomega.1c06272.

EDS data for the metal foam only before and after the reaction (Table S1); EDS data for the HZSM-5 pellet before and after the reaction (Table S2); EDS data for the HZSM-5 coated metal foam before and after the reaction (Table S3); and EDS data for the AC-673 coated metal foam before and after the reaction (Table S2) (PDF)

## ■ AUTHOR INFORMATION


### Corresponding Author

**Jihoon Jung** − *Kyonggi University, Suwon-si, Gyeonggi-do 16227, Republic of Korea;* orcid.org/0000-0001-7370-076X; Email: jhjung@kgu.ac.kr; Fax: +82-1034035568

### Authors

**Jeongin Mun** − *Kyonggi University, Suwon-si, Gyeonggi-do 16227, Republic of Korea*

**Nari Kim** − *Kyonggi University, Suwon-si, Gyeonggi-do 16227, Republic of Korea*

**Byunghun Jeong** − *Agency for Defense Development, Daejeon 34060, Republic of Korea*

Complete contact information is available at: https://pubs.acs.org/10.1021/acsomega.1c06272


### Notes

The authors declare no competing financial interest.

## ■ ACKNOWLEDGMENTS

This research was funded by Grant-in-aid from the Korean Agency for Defense Development (ADD) and was supported by Kyonggi University Research grant 2021.

## ■ REFERENCES

(1) Lander, H. R.; Nixon, A. C. Endothermic fuels for high mach vehicles. *Am. Chem. Soc., Div. Petro. Chem.* **1987**, *32*, 504−511.

(2) Lander, H.; Nixon, A. C. Endothermic Fuels for Hypersonic Vehicles. *J. Aircr.* **1971**, *8*, 200−207.

(3) Edwards, T. Liquid Fuels and Propellants for Aerospace Propulsion: 1903-2003. *J. Propul. Power* **2003**, *19*, 1089−1107.

(4) Kay, I. W.; Peschke, W. T.; Guile, R. N. Hydrocarbon - fueled scramjet combustor Investigation. *J. Propul. Power* **1992**, *8*, 507−512.

(5) Sobel, D. R.; Spadaccini, L. J. In Hydrocarbon fuel cooling technologies for advanced propulsion. *Am. Soc. Mech. Eng.* **1995**, *3*, No. 95-GT-226.
(6) Fan, X. J.; Zhong, F. Q.; Yu, G.; Li, J. G.; Sung, C. J. Catalytic cracking and heat sink capacity of aviation kerosene under supercritical conditions. *J. Propul. Power* **2009**, *25*, 1226−1232.
(7) Huang, H.; Spadaccini, L. J.; Sobel, D. R. Fuel-cooled thermal management for advanced aeroengines. *J. Eng. Gas Turbines Power* **2004**, *126*, 284−293.
(8) Friend, D. G.; Huber, M. L. Thermophysical Property Standard Reference Data from Nist. *Int. J. Thermophys.* **1994**, *15*, 1279−1288.
(9) dos Santos, P. R.; Daniel, L. A. A review: organic matter and ammonia removal by biological activated carbon filtration for water and wastewater treatment. *Int. J. Environ. Sci. Technol.* **2020**, *17*, 591−606.
(10) Park, S.-J.; Kim, Y.-M. Influence of anodic treatment on heavy metal ion removal by activated carbon fibers. *J. Colloid Interface Sci.* **2004**, *278*, 276−281.
(11) Le Leuch, L. M.; Bandosz, T. J. The role of water and surface acidity on the reactive adsorption of ammonia on modified activated carbons. *Carbon* **2007**, *45*, 568−578.
(12) Zawadzki, J.; Wisniewski, M. In situ Characterization of Interaction of Ammonia with Carbon Surface in Oxygen Atmosphere. *Carbon* **2003**, *41*, 2257−2267.
(13) Omar, R.; Robinson, J. P. Conventional and microwave-assisted pyrolysis of rapeseed oil for bio-fuel production. *J. Anal. Appl. Pyrolysis* **2014**, *105*, 131−142.
(14) Suprianto, T.; Winarto; Wijayanti, W.; Wardana, I. Effect of activated carbon catalyst on the cracking of biomass molecules into light hydrocarbons in biomass pyrolysis. *Mater. Sci. Eng.* **2021**, *1034*, No. 012079.
(15) Kostyniuk, A.; Grilc, M.; Likozar, B. Catalytic Cracking of Biomass-Derived Hydrocarbon Tars or Model Compounds To Form Biobased Benzene, Toluene, and Xylene Isomer Mixtures. *Ind. Eng. Chem. Res.* **2019**, *58*, 7690−7705.
(16) Sadeek, S. A.; Mohammed, E. A.; Shaban, M.; Kana, M.T.H.; Negmb, N. A. Synthesis, characterization and catalytic performances of activated carbon-doped transition metals during biofuel production from waste cooking oils. *Mol. Liq.* **2020**, *306*, No. 112749.
(17) Lam, S. S.; Mahari, W.A.W.; Cheng, C. K.; Omar, R.; Chong, C. T.; Chase, H. A. Recovery of diesel-like fuel from waste palm oil by pyrolysis using a microwave heated bed of activated carbon. *Energy* **2016**, *115*, 791−799.
(18) Song, K. H.; Jeong, S. K.; Park, K. T.; Lee, K. Y.; Kim, H. J. Supercritical catalytic cracking of n-dodecane over air-oxidized activated charcoal. *Fuel* **2020**, *276*, No. 118010.
(19) Lee, J. H.; Lee, I. G.; Park, J. Y.; Lee, K. Y. In-situ upgrading of bio-tar over Mg-Ni-Mo catalyst supported by KOH treated activated charcoal in supercritical ethanol. *Fuel* **2019**, *247*, 334−343.
(20) Wickham, D. T.; Atria, J. V.; Engel, J. R.; Hitch, B. D.; Karpuk, M. E.; Striebich, R. Formation of carbonaceous deposits in a model jet fuel under pyrolysis conditions: Structure of jet fuels V. *Am. Chem. Soc., Div. Pet. Chem.* **1998**, *43*, 428−432.
(21) Baker, R. T. K.; Alonzo, J. R.; Dumesic, J. A.; Yates, D. J. C. Effect of the Surface-state of Iron on Filamentous Carbon Formation. *J. Catal.* **1982**, *77*, 74−84.
(22) Reyniers, G. C.; Froment, G. F.; Kopinke, F. D.; Zimmermann, G. Coke formation in the thermal cracking of hydrocarbons. 4. Modeling of coke formation in naphtha cracking. *Ind. Eng. Chem. Res.* **1994**, *33*, 2584−2590.
(23) Edwards, T.; Atria, J. V. Thermal Stability of High Temperature fuels. *Am. Soc. Mech. Eng.* **1997**.
(24) Qu, S.; Liu, G.; Meng, F.; Wang, L.; Zhang, X. Catalytic cracking of supercritical n-dodecane over wall-coated HZSM-5 with different Si/ Al ratios. *Energy Fuels* **2011**, *25*, 2808−2814.
(25) Liu, G. Z.; Zhao, G. L.; Meng, F. X.; Qu, S. D.; Wang, L.; Zhang, X. W. Catalytic Cracking of Supercritical n-Dodecane over Wall-Coated HZSM-5 Zeolites with Micro- and Nanocrystal Sizes. *Energy Fuels* **2012**, *26*, 1220−1229.
(26) Meng, F.; Liu, G.; Qu, S.; Wang, L.; Zhang, X.; Mi, Z. Catalytic Cracking and Coking of Supercritical n-Dodecane in Microchannel Coated with HZSM-5 Zeolites. *Ind. Eng. Chem. Res.* **2010**, *49*, 8977−8983.
(27) Li, J.; Zou, J.; Zhang, X.; Guo, W.; Mi, Z. Catalytic cracking of endothermic fuels in coated tube reactor. *Front. Chem. Eng. China* **2008**, *2*, 181−185.
(28) Mun, J. I.; Jeon, H. Y.; Jeong, B. H.; Jung, J. H. Decomposition of endothermic fuel using washcoated HZSM-5 on metal foam. *Catal. Today* **2021**, *375*, 537−546.
(29) Shin, M. C.; Mun, J. I.; Park, J. H.; Jung, J. H.; Jeong, B. H. Decomposition reaction of methylcyclohexane using H-ZSM-5 supported on NiCrAl metal foam. *React. Kinet., Mech. Catal.* **2019**, *126*, 761−772.
(30) Lei, Z.; Hao, S.; Yang, J.; Lei, Z.; Dan, X. Study on solid waste pyrolysis coke catalyst for catalytic cracking of coal tar. *Int. J. Hydrogen Energy* **2020**, *45*, 19280−19290.
(31) Edwards, T. Cracking and deposition behavior of supercritical hydrocarbon aviation fuels. *Combust. Sci. Technol.* **2006**, *178*, 307−334.
(32) Hoff, T. C.; Thilakaratne, R.; Gardner, D. W.; Brown, R. C.; Tessonnier, J. P. Thermal Stability of Aluminum-Rich ZSM-5 Zeolites and Consequences on Aromatization Reactions. *J. Phys. Chem. C* **2016**, *120*, 20103−20113.
(33) Wojciechowski, B. W. The reaction mechanism of catalytic cracking: Quantifying activity, selectivity, and catalyst decay. *Catal. Rev.: Sci. Eng.* **1998**, *40*, 209−328.
(34) Lemmon, E. W.; Huber, M. L. Thermodynamic properties of n-dodecane. *Energy Fuels* **2004**, *18*, 960−967.


https://doi.org/10.1021/acsomega.1c06272
*ACS Omega* 2022, 7, 8518−8525